

See discussions, stats, and author profiles for this publication at: <https://www.researchgate.net/publication/275026294>

Surface Effects on Photoluminescence and Optical Nonlinearity of CdS Quantum Dots Stabilized by Sulfonated Polystyrene in Water

ARTICLE *in* THE JOURNAL OF PHYSICAL CHEMISTRY C · MARCH 2015

Impact Factor: 4.77 · DOI: 10.1021/jp511777x

READS

66

5 AUTHORS, INCLUDING:



Jolly Antony

Maharaja's College

3 PUBLICATIONS 4 CITATIONS

[SEE PROFILE](#)



Pradeep Chandran

Cochin University of Science and Technology

22 PUBLICATIONS 21 CITATIONS

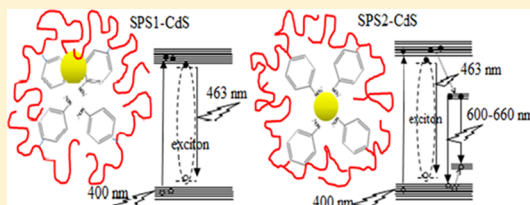
[SEE PROFILE](#)

Surface Effects on Photoluminescence and Optical Nonlinearity of CdS Quantum Dots Stabilized by Sulfonated Polystyrene in Water

Jolly Vakayil Antony,^{†,‡} Pradeep Chandran,[§] Philip Kurian,[†]Nampoori Parameswaran Narayanan Vadakkedathu,[§] and George Elias Kochimoolayil*,^{†,||}[†]Department of Polymer Science and Rubber Technology, Cochin University of Science and Technology, Kerala, 682022, India[‡]Department of Chemistry, Government Brennen College, Thalassery, Kerala, 670106, India[§]International School of Photonics, Cochin University of Science and Technology, Kerala, 682022, India

S Supporting Information

ABSTRACT: A simple aqueous method has been used for the direct synthesis of water-soluble sulfonated polystyrene (SPS) encapsulated CdS quantum dots (QDs). The aqueous solution of the QDs, stabilized by two SPSs of different sulfonation level, shows a blue shift in ultraviolet-visible (UV-vis) absorption and band edge emission. High resolution transmission electron microscope (HR-TEM) establishes the presence of quantum confined CdS particles. The sulfonation level of SPS influences the size of QDs and strongly affects the photoluminescence (PL). The CdS QDs passivated by SPS with less sulfonation level exhibit only band edge emission (463 nm), while QDs in aqueous solution of SPS with high sulfonic acid content emits predominantly defect state emission (610 nm) against the band edge emission (463 nm). The PL of the SPS-CdS nanocomposites demonstrates an interesting variation in emission spectra and quantum yield via the change in sulfonation level, the change in pH and on keeping in aqueous solution. In addition, the z-scan measurements show negative nonlinear refraction coefficient, indicating self-defocusing phenomena. The absolute value of the third order nonlinear refractive index and nonlinear absorption are decided by the CdS QDs surface chemistry.



1. INTRODUCTION

Quantum confined semiconducting nanoparticles, called quantum dots (QDs) possessing unique size and surface nature dependent optical properties have attracted the current research of light induced processes. Synthesis of hydrophobic QDs and their photo optical properties are well established for optoelectronic applications, nonlinear optics, and photocatalysis.^{1–3} Water-soluble QDs and its luminescence originating from surface interaction with the environment have opened a promising window for metal ion sensing applications.⁴ For use as chemical sensors, QDs should be easily synthesized and stabilized in aqueous solution. The photoluminescence (PL) of aqueous CdS QD solution and its dependence on the size, nature of capping ligands, temperature, and pH of the medium have been used for biomolecule labeling and metal ion detection.^{5,6} Although both the size and the surface nature of the QDs determine the luminescence characteristics, ability to tailor the latter is comparatively more important in chemical sensing than the former. It has been a difficult endeavor to study the surface interaction, due to the several experimental difficulties and limited knowledge. However, fluorescence spectroscopy can be used to assess the surfaces and interactions at the QD-ligand nano interfaces in a water medium.⁷ It has been reported that, in aqueous solution, even macromolecular configuration influences the luminescence behavior of QDs.⁸ Synthesis and protection of QDs from aggregation in an aqueous medium is more challenging and is being explored.

Several researchers have succeeded in the synthesis of water-soluble CdS QDs using capping molecules like thioglycolic acid, thioglycerol, cystein, mercaptopropionic acid, and mercaptoundecanoic acid.^{9–11} Hydrophilic polymers, polyethylenimine (PEI), and poly(acrylicacid) (PAA) in ethylene glycol and water solvents, respectively, are also reported to be effective for the direct synthesis of water-soluble CdS QDs.^{12,13} Aqueous route synthesis of water-soluble QDs using polymers is a highly appreciated environment friendly methodology, which is rarely reported and need more exploration.¹⁴

Nonlinear optical properties of CdS QDs incorporated in polymer were reported. Schwerzel et al. and He et al. have studied the optical nonlinearity of CdS QDs embedded in polydiacetylene and nafion, respectively.^{15,2} There has been an extensive need for nonlinear optical materials that can be synthesized and processed easily because of their potential applications in photonic devices. The nonlinear optical properties of semiconductor QDs, including CdS, ZnS, and CdSe, can be tuned by changing the QD size and surface chemistry.¹⁶ z-Scan technique is the most established method to characterize the nonlinear optical properties of materials. Sheikh-Bahae et al. have reported a single beam z-scan method for measuring the sign and magnitude of nonlinear refractive

Received: November 25, 2014

Revised: March 4, 2015

Published: March 24, 2015



ACS Publications

© 2015 American Chemical Society

index (n_2).¹⁷ This method is also extended for the measurement of nonlinear absorption.

Recent advances in water-soluble QDs have given us the freedom to think up better QDs that are cheaper and environment friendly.¹⁸ In a step toward achieving this goal in an affordable way, we have synthesized the SPS from expanded polystyrene waste (PS) and used it as a stabilizer in aqueous solution for the CdS QDs synthesis. The SPS behaves as a water insoluble hydrogel when its sulfonation level (f) < 30%, while it acts as a water-soluble polyelectrolyte when " f " is raised above 30%.¹⁹ Recently, we have published an *in situ* method for the formation of nanocomposite with partially sulfonated polystyrene hydrogel ($f = 30\%$) and CdS QDs. The synthesized water insoluble composite was used for the solar light driven photocatalytic degradation of an organic dye.²⁰ Various applications of polyelectrolyte (SPS) such as, water purification and ion exchange membrane were already reported, but no literature regarding its use as a stabilizer for the QDs in aqueous solution has come to the attention of authors until date. The purpose of this work is to obtain a water-soluble nanocomposite using SPS, $f > 75\%$ and CdS QDs. The SPSs of different sulfonation level are proposed to be achieved by homogeneous and heterogeneous sulfonation of PS. The CdS QDs are generated in an aqueous solution of SPS for the ultimate formation of water-soluble nanocomposite film, which is to be characterized by Fourier transform infrared spectroscopy (FTIR), X-ray diffraction (XRD), and high resolution transmission electron microscopy (HR-TEM). Thermal stability of the SPS and its composite with CdS QDs is compared using thermogravimetric analysis (TGA). Aqueous solution of the film is used for UV-vis absorption and photoluminescence studies. The interesting difference in the emission features of CdS QDs incorporated in differently sulfonated polystyrene is proposed to be highlighted. Also, the NLO properties of the water-soluble SPS-CdS composites are proposed to be investigated using *z*-scan method.

2. EXPERIMENTAL SECTION

2.1. Materials. Expanded polystyrene waste (PS) was used for the synthesis of sulfonated polystyrene (SPS). Analytical reagent grade sulfuric acid (H_2SO_4 , 98%), silver sulfate (Ag_2SO_4), cadmium acetate [$Cd(CH_3COO)_2 \cdot 2H_2O$], calcium carbonate ($CaCO_3$), sodium sulfide ($Na_2S \cdot 9H_2O$), and 1,2-dichloroethane (DCE) were purchased from Merck. Dialysis tubing (Sigma-Aldrich) cut off MW 12000–14000 was used for the purification of aqueous solution of SPS.

2.2. Preparation of SPS1-CdS and SPS2-CdS Nanocomposites. The nanocomposites of CdS QDs were synthesized in aqueous medium with two sulfonated polystyrenes (SPS1 and SPS2) of different sulfonation level. (Experimental details are given in Supporting Information.) The aqueous solutions of the composites, SPS1-CdS and SPS2-CdS, were used for linear and nonlinear optical studies. To analyze the effect of pH on QD formation, the SPS2 composite was prepared in two different pH. The aqueous solution of SPS2 is acidic ($pH = 4$) in which CdS QDs were generated, while the other SPS2 solution was made basic ($pH = 8$) by the addition of 0.1 N NaOH and then CdS QDs were formed. The two composite films of SPS1 and SPS2 were redissolved in water and checked for the precipitation of CdS by keeping the solution for more than one month.

2.3. Characterization. 1H NMR spectra were used to confirm the sulfonation as well as the sulfonation level of SPSs.

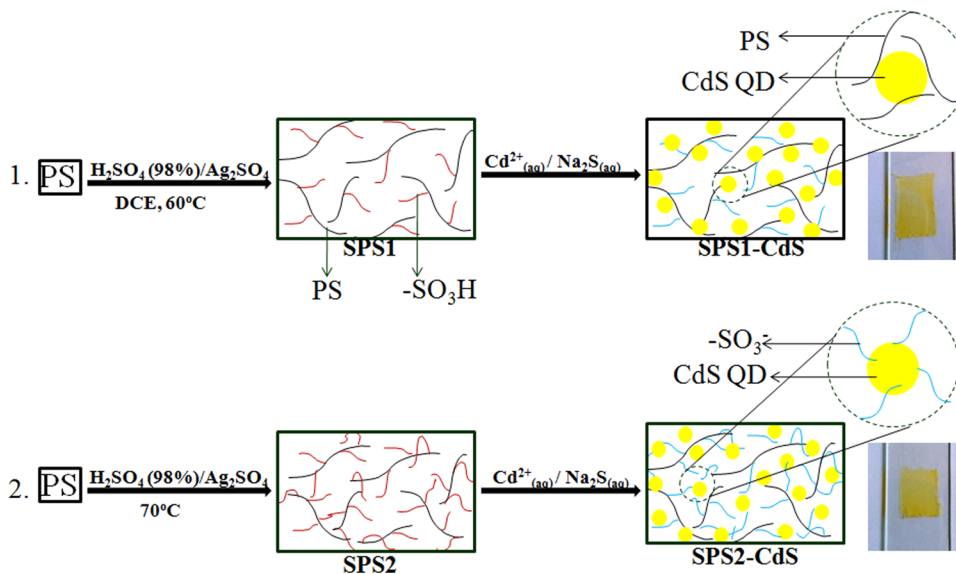
The NMR measurements of SPS1 and SPS2 dissolved in dimethyl- d_6 sulfoxide ($DMSO-d_6$) and PS dissolved in $CDCl_3$ were performed on a Bruker 400 spectrometer (400 MHz). Relative areas of peaks corresponding to aliphatic protons and three types of aromatic protons were obtained from the Bruker spectrometer. The peak areas of aromatic protons were used to calculate the sulfonation level of SPSs.

The aqueous solution of SPS encapsulated CdS QDs can be easily cast to yellow transparent film (SPS1-CdS and SPS2-CdS). Sulfonic acid vibration bands in SPS and its change during the attachment of Cd^{2+} ions and CdS formation was studied using Thermo Nicolet Avatar 370 FT-IR spectrometer. KBr pellet was prepared using the cracked pieces of the sample film and scanned in the range 400 to 4000 cm^{-1} . Powder X-ray diffraction of the composite film was carried out on Bruker AXS D8 Advance diffractometer equipped with graphite monochromated Cu $K\alpha$ radiation ($\lambda = 1.5406 \text{ \AA}$) in the 2θ range from 10° to 80° . Debye-Scherrer formula was used to calculate the average crystallite size.²¹ A High Resolution Transmission Electron Microscope (HR-TEM) JEOL 3010 operated at an accelerating voltage of 300 kV ($Cs = 0.6 \text{ mm}$, resolution 1.7 \AA) was used to analyze the size of nanocrystals. Composite film was dissolved in water and a drop of the solution was placed on a 200 mesh copper grid coated with carbon film. This was subsequently dried under vacuum and loaded in the electron microscope chamber. The composite film was suspended in tetrahydrofuran (THF), which is a nonsolvent and the suspension was also used for HR-TEM analysis. ImageJ software was used to analyze the HR-TEM image for the determination of particle size and crystal plane spacing. TGA/differential thermal analysis (DTA) was used to compare the thermal stability of SPS and SPS-CdS using universal TA Instruments Q50 analyzer. Samples of about 6 mg were heated from 25 to 700 °C at 10 °C/min in nitrogen atmosphere.

2.4. Optical Properties. The SPS-CdS composite films were redissolved in water for UV-vis absorption measurements using Shimadzu UV-vis spectrophotometer. A portion of the aqueous solution of films was kept for 3 h. This is to identify any possible change in the absorption of CdS QDs on standing in aqueous medium. Also, the aqueous solution of the CdS QD composites prior to film casting (solution at the time of CdS QD formation) was used for UV-vis absorption. Absorption spectrum of the composite films (on glass slides) was also taken using Varian Carry 5000 UV-vis spectrophotometer. Absorption onset (λ_e) and absorption maximum (λ_m) were obtained by drawing tangents on the sharply decreasing region of the absorption spectra of the CdS QDs.²² Hnglein's empirical equation was used to calculate the size range of CdS particles in the composite film and the result is compared with the size obtained from HR-TEM.²² The steady state photoluminescence spectrum of the CdS QDs in water at three different stages (at the time of CdS QD formation in aqueous solution, after film casting and on standing the QD film solution for 3 h), as used for the UV-vis absorption, was taken in the wavelength range of 410–800 nm using FluoroMax-3 spectrofluorimeter. The excitation wavelength of 400 nm was used for the luminescence studies. The absorption and fluorescence spectra of CdS QDs in aqueous solution of SPS2 in acidic ($pH = 4$) and basic medium ($pH = 8$) were also taken to verify the absorption and fluorescence dependence on pH.

2.5. Nonlinear Optical Properties. Nonlinear optical measurements were carried out employing *z*-scan technique using a mode-locked Nd:YAG laser having 7 ns pulses at a

Scheme 1. Illustration for the (1) Homogeneous Sulfonation, Followed by SPS1-CdS Formation; (2) Heterogeneous Sulfonation, Followed by SPS2-CdS Formation



repetition rate of 10 Hz giving a second harmonic at 532 nm. The two composite films (SPS1-CdS and SPS2-CdS) were dissolved in water and the aqueous solutions were used for z-scan measurements. The sample was moved along the beam axis of light focused with a lens of focal length 20 cm. In closed aperture (CA) z-scan measurements, an aperture was placed between the sample and the detector, allowing the determination of nonlinear refraction (NLR). The beam waist (w_0) of the laser pulse was calculated to be $42 \mu\text{m}$. The Rayleigh length, $z_0 = \pi w_0^2 / \lambda$, is estimated to be 10.7 mm, which is much greater than the thickness of the sample cuvette (1 mm). In open aperture (OA) z-scan, the beam is totally collected by a large diameter lens, for the determination of nonlinear absorption (NLA). The spectra of normalized transmittance versus sample distance (z) from the focus were plotted. The NLR and NLA coefficients, n_2 and β , for the CdS QDs in water were determined from the fitting of experimental curves.

3. RESULTS AND DISCUSSION

3.1. Synthesis of SPS1, SPS2, SPS1-CdS, and SPS2-CdS. The reagent H_2SO_4 in the presence of Ag_2SO_4 catalyst has been used for the preparation of SPS1 and SPS2 by homogeneous and heterogeneous sulfonation, respectively. Although the sulfonated polystyrenes (SPS1 and SPS2) obtained by the two methods are soluble in water, they show difference in the easiness of solubility. The SPS2 dissolves very easily in water but SPS1 dissolves only after prolonged stirring. This clearly indicates the difference in their sulfonation level. The SPS2 contains more $-\text{SO}_3\text{H}$ ionic functionals than the SPS1. The aqueous solution of SPS1 and SPS2 forms water-soluble transparent films once the water is evaporated off under ambient conditions. The transparent films of SPSs were redissolved in water and used for the composite preparation. When CdS QDs form, the clear aqueous solution of SPSs becomes yellow. The solution remains as such for more than one month without any CdS precipitation. This shows that SPS1 and SPS2 are effective stabilizers for the water-soluble CdS. The aqueous solution of SPSs stabilized CdS QDs forms yellow composite films, SPS1-CdS and SPS2-CdS. However, it is noteworthy to mention the fact that precipitation of yellow

CdS from the polymer solution was found to occur when the solution was kept for several months. Aqueous routes for the CdS QDs synthesis using the SPS1 and SPS2 are illustrated in Scheme 1.

3.2. Characterization. The ^1H NMR spectra confirm the sulfonation of PS and reveal the level of sulfonation in the two SPSs. The sulfonation to a level of 76% was achieved in SPS1 as per our previous work.²⁰ The PS was sulfonated almost completely, as evidenced from ^1H NMR spectrum of SPS2 (Figure S1, Supporting Information). Figure 1 displays the

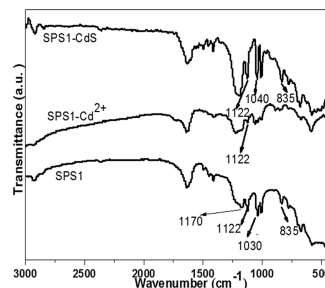


Figure 1. FTIR spectra of SPS1, Cd^{2+} attached SPS1, and SPS1-CdS.

FTIR spectra of SPS1, Cd^{2+} attached SPS1, and SPS1-CdS composite that give evidence for the presence of $-\text{SO}_3\text{H}$ functional groups and incorporation of CdS QDs in the SPS1. Vibrational peaks at 1030 cm^{-1} , 1122 and 1170 cm^{-1} are assigned to stretching vibration of the sulfonic acid functional groups.²³ Substitution at para position is confirmed from the peak at 835 cm^{-1} . The considerable decrease in these vibrational peaks after Cd^{2+} attachment suggests the coordination of Cd^{2+} ions to the sulfonic acid functionals. The regeneration of sulfonic acid peaks after the CdS formation, clearly shows the detachment of CdS QDs from the $-\text{SO}_3\text{H}$ ionic functionals. FTIR spectra of the SPS1 and its composite film show the existence of ionic functional groups even after the formation of CdS QDs and render the film easily soluble in water.

The X-ray diffractogram of the two CdS QD composites in Figure 2 shows the preferential growth of CdS cubic crystal

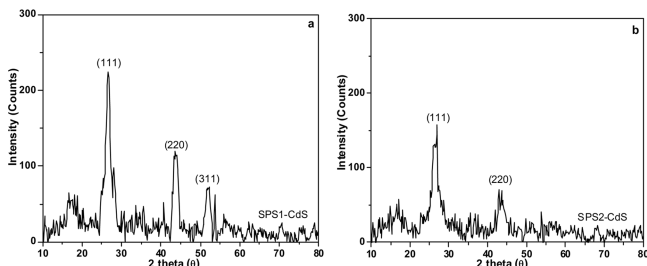


Figure 2. XRD patterns of (a) SPS1-CdS and (b) SPS2-CdS.

phases over hexagonal. The broadened diffraction peaks confirm the nanocrystallinity of CdS. In SPS1-CdS, the diffraction from the (111), (220), and (311) cubic crystal planes is observed as peaks at 2θ values of 26.4° , 43.9° , and 52.1° , respectively.²⁴ The SPS2-CdS gives diffraction peaks from the (111) and (220) planes, which are more broadened than the SPS1 composite and the diffraction from (220) planes are weak to observe. This accounts for the presence of small CdS nanocrystallites in the SPS2 composite than the SPS1 composite. The average sizes of CdS crystallites are found to be 4.3 and 3.8 nm in the SPS1 and SPS2 composite films. The emergence of weak shoulders on either side of (111) diffraction peak show the presence of hexagonal crystal phases of CdS in minor quantity. These weak peaks are observed at 2θ of 25° and 28.3° due to the diffraction from (100) and (101) planes.^{25,26}

The CdS QD size and its distribution in the composite films are investigated using HR-TEM images (Figure 3a–f).

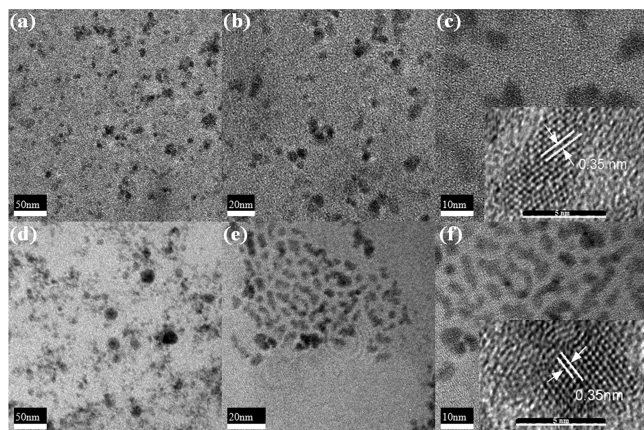


Figure 3. HRTEM images of (a–c) SPS1-CdS and (d–f) SPS2-CdS. Inset: Crystal lattice plane spacing.

The SPS1-CdS and SPS2-CdS films show the presence of CdS QDs of size less than 6 nm, exciton Bohr diameter of bulk CdS. The CdS QDs of size 5.4 ± 1.5 and 4.6 ± 1.5 nm are present in the two composites respectively (Size is taken as the average of 50 particles in the TEM image). High resolution images (inset) show the lattice spacing, $d = 0.35$ nm for the two composites, which corresponds to the (111) cubic crystal plane.²⁵ On correlating HR-TEM with XRD, it is obvious that CdS crystallites are smaller than QDs because two or more crystallites combine to form QDs. The crystal lattice plane spacing and angle of diffraction of CdS QD confirm its cubic

crystal structure. The images at low resolution show the uniform distribution of CdS QDs along with aggregated particles. Although coalescence of QDs is very high in water, the SPS is capable enough to stabilize the CdS QDs in the major areas of the composite film. The composite films of SPS1-CdS and SPS2-CdS, from its aqueous solution were originally obtained in 1 h at 70°C . During HR-TEM imaging, the composite film was redissolved in water and recast on copper grid of the instrument in 24 h at room temperature under vacuum. Recasting of composite film on the copper grid using water gives an additional chance for aggregation at certain regions of the composite film. Previously the agglomeration of QDs has been reported even in coordinating solvents such as DMF using partially sulfonated polystyrene.²⁷ The composite films can be directly analyzed without recasting to confirm the presence of quantum confined CdS in the film. With that intention the two composite films are fragmented to fine pieces in THF and analyzed using HR-TEM. The composites form a suspension from which the composite pieces settle down. The supernatant solution which contains very fine film pieces is used for the analysis. The CdS QDs are distributed uniformly in polymer SPS2 (Figures S2 and S3). The size of the QDs is obtained as 3.8 ± 0.7 , which is well below the QD size that is obtained by casting the film using water. This confirms the possible aggregation of CdS QDs during recasting of film using water. The size CdS QDs present in SPS1 is 6.5 nm and is same as that obtained earlier by dissolving film in water. This shows that aggregation of CdS has been occurred during the initial film casting itself because of the weak stabilization of QDs by SPS1 (Figures S2 and S3 and details are in Supporting Information).

Thermal stability of the SPS1, SPS2, and their CdS QD composites are compared in Figure 4a,b. Since SPS1 and SPS2

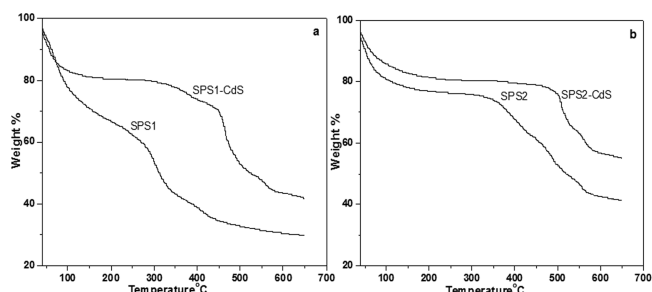


Figure 4. TGA curves of (a) SPS1 and SPS1-CdS composite (b) SPS2 and SPS2-CdS composite.

are water absorbing, the initial weight loss of 20 and 10%, respectively, at around 100°C is due to the removal of water. The thermograms of the composites with respect to their polymers confirm that the composites are thermally stable. The thermal degradation of the composites has happened at high temperature compared to the respective polymers. The incorporation of inorganic compounds in polymer materials enhances the thermal stability of the polymer. The aromatic ring and $-\text{SO}_3^-$ groups in the SPS chains make coordinate linkages with the CdS. This interfacial attraction restricts the thermal motion of the SPS molecules and reinforces the polymer chains for a stable nanocomposite. Similar thermograms were obtained earlier for polymer–semiconductor nanocomposites.²⁸ The residual weights of the SPS1 and its composite are 30 and 42%, respectively, whose difference

corresponds to the inorganic content in the composite. This is used for the approximate calculation of the CdS content in the nanohybrid.²⁸ Thus, the SPS1-CdS composite consists of 17% by weight of CdS. The residual weights of the SPS2 and its CdS QD composite are 41 and 55%, respectively. This shows the existence of 24% by weight of CdS in SPS2-CdS. The highly sulfonated polystyrene (SPS2) can hold more amount of CdS.

3.3. Optical Properties. The UV-vis absorption and photoluminescence spectra give credence to the presence of quantum confined CdS particles in the composite films. The UV-vis absorption spectra of the SPS2 film, CdS QD composite film of SPS1 and SPS2, and their aqueous solutions are presented in Figure 5a,b.

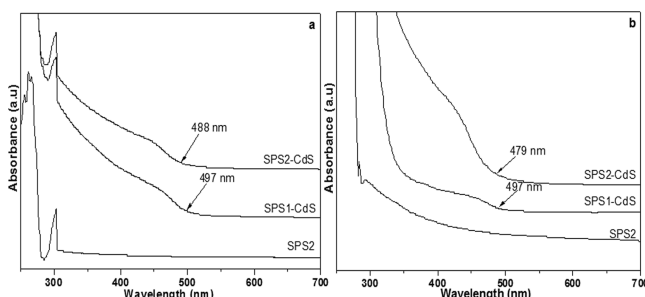


Figure 5. UV-vis absorption spectra of (a) SPS2, SPS1-CdS, and SPS2-CdS film dissolved in water (b) SPS2, SPS1-CdS, and SPS2-CdS film.

The SPS2 absorbs in ultraviolet region, while the CdS QD composites of SPS1 and SPS2 absorb in the visible region characteristic of CdS QDs with absorption onset (λ_e) and absorption maximum (λ_m).²⁹ Since the CdS particles are quantum confined, the λ_e and λ_m of the exciton band is a function of QD size. The Henglein's empirical equation relates the diameter ($2R_{\text{CdS}}$) of the particle to the λ_e or λ_m , which is used to find the size distribution of particles that lie within the quantum confined regime.³⁰ The aqueous solution of the films, the CdS QDs protected by SPS1 and SPS2 show onset of absorption at 497 and 488 nm (Figure 5a), which correspond to a size of 5.8 and 5.2 nm, respectively. The SPS2 solution at pH of 8 stabilizes CdS QDs of size 5.5 nm with an absorption edge at 493 nm (Figure S4, Supporting Information). The pH of SPS2 solution has no significant effect on the absorption edge. The absorption onset and therefore the CdS QD size in the film (Figure 5b) and its solution are exactly same for SPS1-CdS, while SPS2-CdS film on dissolution in water shows a minor red shift in absorption. This may be due to the experimental error as two different spectrophotometers are used for the film and solution analysis or due to the unavoidable aggregation of CdS in water. These QDs, whose size are calculated using λ_e , form the higher end of the particle distribution in the composites.²² The size of the CdS QDs, calculated using Henglein's empirical equation, is correlated to the HR-TEM images of the composites. However, the images show the existence of smaller particles that correspond to the λ_m and aggregated CdS particles that are formed during the recasting of film on copper grid using water. A blue shift in the absorption onset relative to bulk CdS (515–520 nm) supports the quantum confinement effect in the CdS nanocrystals.³¹ The composites have shown slight difference in their blue shift which can be correlated to the relative size and stability of QDs within the two differently sulfonated polystyrene. The large

blue shift in SPS2 composite film and its solution reveals that although the ionic functional group aggregate is larger in SPS2, the size of CdS QD is small compared to SPS1 composite film. This is against the reports of CdS QDs synthesized in hydrophilic polymer micelle, where micelle size decides the size of nanocrystals.³⁰ The proposed mechanism for this peculiar behavior of the composites is explained in the following section.

Inorder to compare the stability of CdS QDs in water, the relation between the absorption edge and size at different stages after its formation is presented in Table 1. (See the absorption

Table 1. Parameters of CdS QDs Protected by SPS1 and SPS2 in Aqueous Solution

sulfonated polystyrene	λ_e^a (nm)	$2R_{\text{CdS}}^a$ (nm)	λ_e^b (nm)	$2R_{\text{CdS}}^b$ (nm)	λ_e^c (nm)	$2R_{\text{CdS}}^c$ (nm)
SPS1	480	4.7	497	5.8	493	5.5
SPS2	490	5.3	488	5.2	487	5.1
SPS2 in basic medium	494	5.6	493	5.5	493	5.5

^aAt the time of CdS QD formation in aqueous medium. ^bAfter film casting. ^cAqueous solution of QD on standing for 3h.

peaks, Figures S5 and S6 in Supporting Information.) The exciton absorption of SPS2 encapsulated CdS QDs in aqueous solution remains unchanged, while a significant change is observed in SPS1 stabilized QDs. The sulfonic acid ionic clustering within the polymer matrix has provided a confined region for particle growth. In SPS1 solution, CdS precipitate within the small ionic core for small size QDs. During film casting or keeping for hours in aqueous solution, the CdS QDs are detached from the ionic core and gets passivated by the polymer chains. The size of detached CdS QDs has increased due to aggregation, which is reflected as a red shift in absorption. The ionic core of SPS2 is comparatively large to precipitate CdS QDs of relatively large size. However, the absorption onset of SPS2-CdS composite is not affected on long-standing in aqueous solution or during film casting. The consistency in absorption peaks of the CdS at different stages after its preparation have shown that the QDs are well stabilized in the aqueous solution of SPS2. The large number of sulfonic acid functionals in SPS2 direct the CdS particles toward the core of the ionic functionals and the particles are always within the clinches of ionic cluster, so that the SPS2 can more efficiently stabilize the QDs than SPS1. During this analysis, for a given composite the absorption spectra at different dilutions have been taken. Although the absorption wavelength remains same for different concentrated solutions of a composite there is a slight change in absorption onset (determined by drawing tangents). The absorption onsets give different size for CdS QDs in a composite. The maximum blue-shifted absorption onset is used for CdS QD size calculation and is tabulated in Table 1. Average size of CdS QDs in a composite and its standard deviation is given in Table S1 (Supporting Information).

PL spectra of the composite films are given in Figure 6. (PL of SPS2, Figure S7, is given in Supporting Information.) The SPS1 composite exhibits near band edge emission at 463 nm, while SPS2 composite shows defect state broad emission of 610–660 nm at the expense of direct band gap electronic emission (463 nm). Asymmetry in band edge luminescence peak of SPS1-CdS is due to a weak shoulder at long wavelength

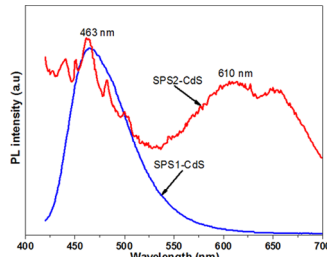


Figure 6. PL spectra of SPS1-CdS and SPS2-CdS composite films in water excited by 400 nm.

region around 512 nm, which corresponds to a defect state emission. The wavelength of emissions (band edge and trap states) observed for the composites are characteristic of CdS QDs.¹² The significant difference in luminescence is accorded to the surface passivation rather than nanocrystal size because the two systems exhibit same position of band edge emission (463 nm). The band edge emission peaks of the CdS QDs, usually assigned to recombination of excited state excitons, have blue-shifted relative to bulk CdS.⁷ This is in accordance with the blue shift in absorption edge of the two composites. The excited electrons in SPS2-CdS get trapped in deep defect state levels of sulfur vacancy. They recombine with holes in the valence band and holes in the trap states near the valence band for a deep trap emission.³²

Although the λ_e of the QDs in SPS1 and SPS2 show minor difference, the position of band edge luminescence (463 nm) exhibited by the QDs are same in the two solutions. The consistency in band edge emission peaks of the two composites can be explained on comparing PL peak broadness and the difference between the λ_e values of the two composites. The minor difference in the size of CdS QDs or in the absorption onset is not significant enough to produce a spectral shift in the band edge emission. Width of the band edge emission is large compared to the difference in the absorption edge of the CdS QDs stabilized by SPS1 and SPS2. But the two composites show an interesting difference in the PL because the sulfonation level of SPS has a strong influence on the intensity of band edge luminescence against defect state emission of CdS QDs. Composite formation has been triggered by the aggregation of Cd^{2+} ions in the core of ionic functional groups. In SPS1-CdS composite, the CdS particle formation weakens the ionic bonding between the $-SO_3^-$ and Cd^{2+} ions, thus, detaching the particles from ionic functionals. The detached CdS QD are stabilized within the polymer network and surface is passivated by the polymeric chain. This minimizes the surface defects thus exhibiting fluorescence mainly due to exciton recombination with a very weak shoulder of shallow trap emission at around 512 nm.³³ However, due to the extensive sulfonation in SPS2, the CdS particles are retained within the ionic aggregates of $-SO_3^-$. The ionic functional interaction with the CdS particles creates dense surface trap states on the surface of nanocrystals. The composite solution shows predominant defect state emission at the cost of band edge emission. Amelia et al. have demonstrated the recovery of defect state levels in CdS QDs due to the electrostatic interaction with proteins.¹¹ In our previous study, partially sulfonated polystyrene (hydrogel) with more ionic functionals form water insoluble CdS QD composite showing both band edge and surface defect state emission. Less sulfonated hydrogel passivates the CdS QDs to eliminate the defect state levels for its band edge emission.²⁰

Wang et al. have demonstrated that the CdS QD surface interaction with $-COOH$ functional groups creates surface defect state emission, which recedes for band edge emission once the carboxyl functional groups are neutralized.³⁴

Figure 7a,b demonstrates the change in luminescence of QD composites on standing in aqueous solution.

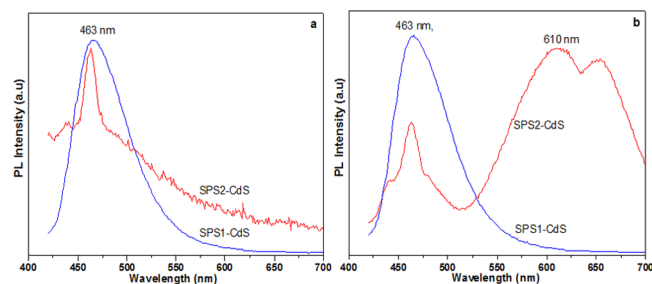


Figure 7. PL spectra of SPS1-CdS and SPS2-CdS composite in water excited by 400 nm (a) at the time of CdS formation and (b) composite film solution on standing for 3 h.

The luminescence position and intensity of SPS1-CdS remains unaltered even after 3 h of standing in aqueous solution (Figure 7a,b) or on film casting (Figure 6). The composite shows band edge emission at 463 nm with a weak shoulder at long wavelength (512 nm). But the luminescence of CdS QDs stabilized by SPS2 has followed a transition from high energy emission to a low energy emission, allowing it to be correlated to change in surface contact between QDs and ionic functional. The composite on standing in aqueous solution, CdS QDs get enough time to be covered by $-SO_3^-$ ionic groups. The enhanced ionic interaction is responsible for the defect state levels in the band gap for the exhibition of defect state emission. PL of CdS QD composite with sulfonated polystyrene of sulfonation level in between that of SPS1 and SPS2 is also studied (Synthesis details of this composite are given in Supporting Information.) This is to ascertain the mechanism proposed for the change in luminescence intensity of SPSs stabilized CdS QDs in water with sulfonation level and on keeping in aqueous solution. The emission behavior is shown in Figure 8a–c and is similar to that observed in SPS2-CdS QD composite with band edge and defect level luminescence. As expected, the luminescence intensity is intermediate to that of SPS1-CdS and SPS2-CdS. This supports the role of sulfonation level on PL intensity. Further it also account for the change in PL intensity of CdS QDs at different stages after its preparation.

The SPS2-CdS synthesized in basic medium also have the same characteristics (Figure 9a–c). During the initial stage of CdS formation, the ionic functionals are in contact with Cd^{2+} ions and eventually the Cd^{2+} ions converts to CdS nanocrystals, whose surface is in interaction with $-SO_3^-$ ionic groups. Initially the CdS surface has no direct contact with ionic functional and with the complete formation of CdS, QDs surface are completely within the ionic shell. The ionic interaction creates dense surface defect state levels that suppress the direct electron–hole recombination to create an emission at 610 nm. The CdS QDs synthesized using aqueous SPS2 solution of pH = 8, have an intense luminescence at 610 nm attributed to the high density of defect states in CdS (Figure 9c). A dramatic increase in the relative intensity of defect state emission compared to band edge emission suggests an increase in the trap states through the increased electrostatic

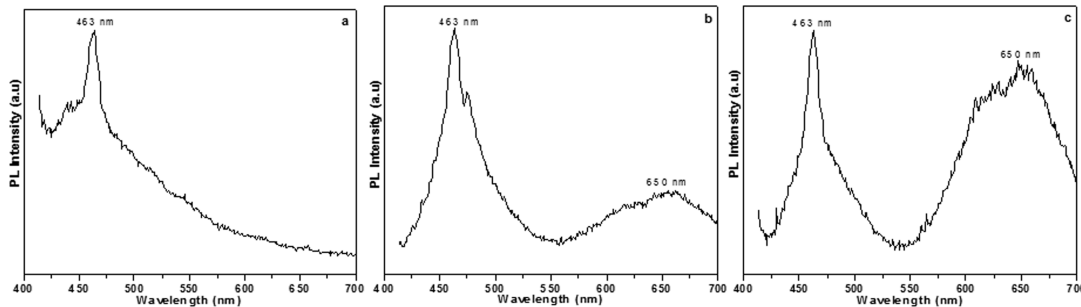


Figure 8. PL spectra of CdS QD composite with SPS of sulfonation level in between SPS1 and SPS2 (a) at the time of CdS QD formation, (b) composite film in water, and (c) composite film solution on standing for 3 h.

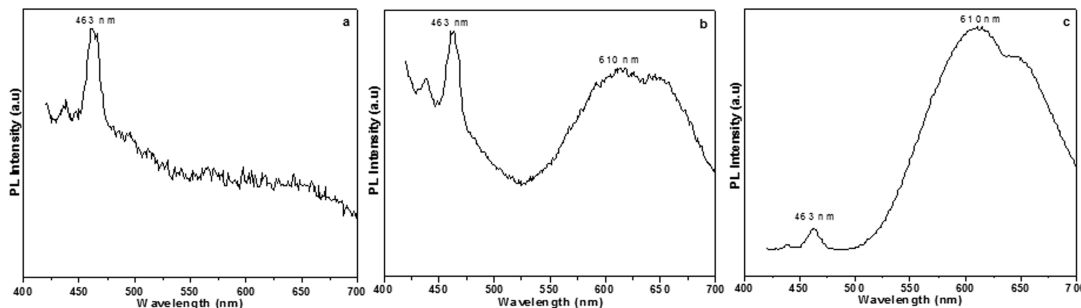


Figure 9. PL spectra of SPS2-CdS composite (synthesized in basic medium) in water excited by 400 nm (a) at the time of CdS formation, (b) SPS2-CdS composite film, and (c) SPS2-CdS film solution on standing for 3 h.

interaction between ionic groups ($-SO_3^-$) and QD surface. The basic medium ionizes the $-SO_3H$ functionals to create more ionic interaction with QD surface. High rise in the baseline around 400 nm region in the fluorescence spectra is due to the mixing of the fluorescence emission with excitation wavelength (Figure 9a,b). In Figure 9c, the fluorescence emission in the 463 nm is very low in comparison with that at 610 nm and, hence, the spectrum starts with the baseline.

The quantum yield (QY) of defect state emission, luminescence peak maximum in the wavelength region 610–650 nm, with respect to rhodamine 6G is zero for SPS1-CdS at different stages of its preparation. But CdS QD composites with SPS2 and sulfonated polystyrene of sulfonation level in between that of SPS1 and SPS2 give defect state luminescence QY. The QY changes on keeping composite film solutions for several hours and is shown in Table 2. The QYs are comparable to CdS QDs synthesized by various other methods reported previously.³⁵

The change of surface defect state brought by the change in surface environment results in the luminescence modulation. The luminescence property of the composites are found

to be distinctly different due to the ionic interaction between the QDs and SPS, which is decided by the sulfonation level. The interacting surface environment dependent luminescence may extent the use of water-soluble CdS QD hybrid in chemical sensors. Easy casting of yellow transparent composite film from the composite solution allows it to use in optoelectronic devices like optical switches based on its nonlinear optical properties.

3.4. Nonlinear Optical Properties. To estimate the nonlinearity of the composites, we have performed CA and OA z-scan on the aqueous solution of SPS1-CdS and SPS2-CdS composite films. The nonlinear optical mechanism results in change in refractive index of the SPS1-CdS and SPS2-CdS composites, which can be evaluated from the transmittance output from a closed aperture z-scan. The normalization is performed in such a way that the transmittance is unity for the sample far from the focus where the nonlinearity is negligible. A self-defocusing nonlinearity results in a peak followed by a valley in the normalized transmittance as the sample is moved away from the lens (Figure 10). The scatter dots are experimental data while the solid lines are theoretically fitting curves by employing standard z-scan theory.¹⁷

The experimental data is best fitted with two photon absorption (TPA) theoretical model and the TPA process is responsible for the nonlinearity of the composites. The symmetrical peak–valley curves were obtained for the two composites, which is due to the fact that the nonlinear refraction is negative and the closed aperture measurement is not sensitive to detect the nonlinear absorption of the composites. The sign and magnitude of the nonlinear refraction are easily deduced from the transmittance curve (z-scan).¹⁷ In a circularly symmetric laser beam incident on the composite, the normalized transmittance detected in far field in the closed aperture is given by eq 1.³⁶

Table 2. Relative PL QYs (ϕ_{Cds}) of Defect State Emission in the Wavelength Range 610–650 nm

ϕ_{Cds}^a	ϕ_{Cds}^b	ϕ_{Cds}^c
zero ^d	0.0065 ^d	0.0238 ^d
zero ^e	0.0122 ^e	0.0629 ^e
zero ^f	0.0188 ^f	0.2615 ^f

^aAt the time of CdS QD formation in aqueous medium. ^bAfter film casting. ^cAqueous solution of QD on standing for 3 h. ^dCdS QD composite with sulfonated polystyrene of sulfonation level in between that of SPS1 and SPS2. ^eSPS2-CdS. ^fSPS2-CdS synthesized in basic medium.

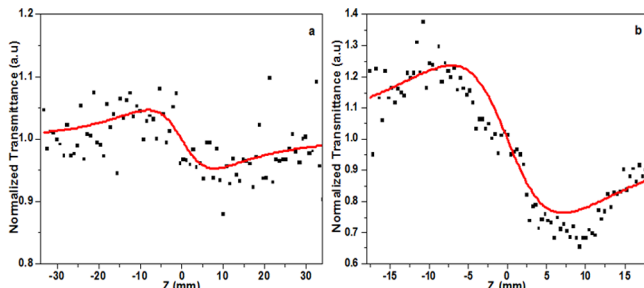


Figure 10. Closed aperture z -scan of (a) SPS1-CdS and (b) SPS2-CdS in water at an incident intensity (I_0) of 0.32 GW/cm^2 .

$$T(z) = 1 - \frac{4\Delta\Phi_0\gamma}{(1 + \gamma^2)(9 + \gamma^2)} \quad (1)$$

where $\Delta\Phi_0 = 2\pi(n_2I_0(t)L_{\text{eff}}/\lambda)$ with $\gamma = (z/z_0)$ and $L_{\text{eff}} = (1 - \exp(-\alpha l))/\alpha$, $\Delta\Phi_0$ being the phase distortion at the focus, I_0 the incident laser power at the focus, L_{eff} the effective interaction length and l the sample length. z and z_0 are the longitudinal displacement of the sample from focus and the Rayleigh length, respectively. The fitting results were used to calculate the third order nonlinear refractive index (n_2). The nonlinear refractive index of the SPS1-CdS and SPS2-CdS is determined as -6.0716×10^{-5} and $-3.07 \times 10^{-4} \text{ cm}^2/\text{GW}$. The exhibition of nonlinearity by the two composites is due to the existence of CdS QDs in the composite as the SPS alone does not show nonlinearity.²⁷ The magnitude of nonlinear refractive indices of the CdS QDs in the composites is comparable with the results obtained for CdS QDs in partially sulfonated polystyrene.²⁷ But the values are less than that of bulk CdS, which had been determined at 532 nm , is because of the enhanced band gap energy of CdS QDs.^{37,38} The size and surface defect state levels of CdS QDs in the composites are different and they have an influence on the optical nonlinearity. Wang et al. have explained the phenomenon of localized field that decrease the nonlinear refractive index as the size of the QDs changes from bulk to QDs and further decrease in QD size.³⁹ In the present study, on the contrary the CdS QDs in SPS2 of smaller size shows enhanced nonlinear refraction than CdS QDs in SPS1. The surface of CdS QDs is in vicinity of SPS1 polymer chains, while the ionic functionals of SPS2 are in intimate contact with the QDs. This difference in the CdS QD surface chemistry is due to the difference in the extent of ionic functionals as evidenced from the PL spectra of the two composites. While the CdS in SPS1 is free of defect state levels, the other possess defect state levels. The nonlinear refractive index of the composites is affected by the defect state levels.²⁷ So the difference in the magnitude of nonlinear refractive index is due to the surface chemistry rather than the size of QDs. Moreover, the CdS QDs are directly attached to the SPSs and the extent of sulfonation in SPS has affected the surface properties.

Open aperture z -scan technique measures the nonlinear absorption of the two composites in water. Figure 11a,b shows the plot related to OA z -scan experiment of the SPS1-CdS and SPS2-CdS composites. There is an obvious difference in the measured NLA for CdS QDs stabilized by SPS1 and SPS2. Transmittance decreases as the sample move toward the focus is attributed to reverse saturable absorption (RSA). With the increase of input fluence saturable absorption (SA) neutralizes the RSA and crossover from RSA to SA occur at the focus. The

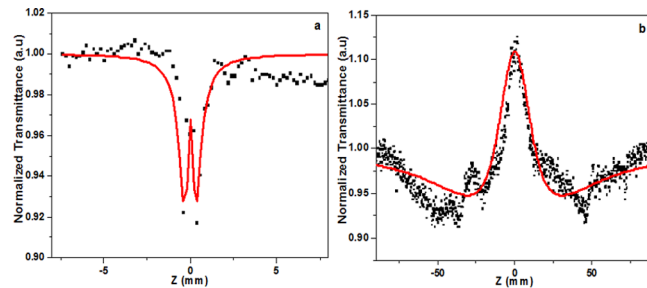


Figure 11. Open aperture z -scan of (a) SPS1-CdS and (b) SPS2-CdS in water at an incident intensity (I_0) of 0.32 GW/cm^2 .

composites exhibit RSA behavior around focus and SA behavior at the focus. This indicates the presence of more than one type of nonlinear optical processes in the composites. Such multiple nonlinear absorption processes were reported by various groups in different materials.^{40–42} Since the composites exhibit RSA and SA behavior the effective nonlinear absorption coefficient, $\alpha(I)$ contains two terms. The first describing the SA and other represent the two photon absorption.⁴³

$$\alpha(I) = \left(\frac{\alpha_0}{1 + I/I_s} + \beta I \right) \quad (2)$$

where α_0 is the unsaturated linear absorption coefficient at the excitation wavelength, I being the incident laser intensity and I_s the saturation intensity. The normalized transmittance of the open aperture z -scan is given by the equation

$$T(z) = \sum_{m=0}^{\infty} \frac{(-\alpha I_0 L_{\text{eff}}/1 + \gamma^2)^m}{m + 1} \quad (3)$$

where the effective interaction length, $L_{\text{eff}} = (1 - \exp(-\alpha l))/\alpha$, I_0 is the irradiance at the focus, and l the sample length; $\gamma = (z/z_0)$, where z and z_0 are the longitudinal displacements of the sample from focus and Rayleigh length, respectively. Theoretical fit of the experimental data was obtained using the eqs 2 and 3 from which β is calculated as -7.972×10^{-13} and $-2.411 \times 10^{-12} \text{ m/W}$, respectively, for the two composites. In SPS1-CdS, as the sample approaches the beam waist, the transmittance has decreased rapidly indicates RSA. A minor flip in the nonlinear absorption curve at the focus manifests the existence of SA. Although the SPS2-CdS also exhibit the same behavior, the SA effect is much larger than that in SPS1-CdS. The difference in relative intensity of RSA and SA behavior in the two composites is due to the difference in the density of surface defect state levels as a consequence of ionic interaction in SPS encapsulated CdS. A large RSA to SA flip at the center for SPS2-CdS has been explained as due to the exciton bleaching in the presence of surface defects.⁴⁴ A strong SA in aqueous solution of SPS2-CdS is accounted to the saturation of absorption from ground state levels including the surface defect state levels, which is absent in SPS1-CdS. There have been reports of SA to RSA and RSA to SA flip at the focus when deoxyribonucleic acid (DNA) is in interaction with Rhodamine 6G and Picogreen dye, respectively.^{43,45} In SPS2-CdS, bleaching of excitonic absorption owing to the presence of defect state level carriers on the CdS QD surface attributes to the occurrence of absorption saturation in laser beam of low intensity. While CdS QD passivated by SPS1 is free of defect state levels for a weak saturable absorption using laser beam of high intensity. The presence of trapped electrons and holes can

modify the liner and nonlinear optical properties.³⁹ An obvious protuberance in the transmission valley with the fluence as in our samples has been observed in metal cluster.⁴⁰

Further z-scan studies are needed to better understand the effect of sulfonation level on the optical nonlinearity. In the present NLO studies of the two composites, it is interesting to know that the surface interaction of the QD with ionic functionals play an important role in NLR and NLA. The NLR can be changed and the NLA can be flipped by adjusting the surface affects of SPS stabilized QDs in water. The large surface to volume ratio of CdS QDs, which are in direct contact with SPS allows the surface properties to strongly influence the nonlinearity. The sulfonation level of the SPS that encapsulate the CdS QDs is an important aspect when these materials are considered for photonic applications. The presence of RSA and SA in the composite could find application in optical switching.

4. CONCLUSION

A novel method has been used for the synthesis of water-soluble CdS QDs using sulfonated polystyrene. The CdS QDs are directly synthesized in water using SPS1 and SPS2. The composite aqueous solution can be easily cast to transparent yellow film. The comparison between the sizes of CdS QDs calculated using absorption onset and HR-TEM images for the two composite films indicates reasonable agreement. Furthermore, blue shift in band edge emission corroborates the existence of QDs in the films. The water-soluble composite film exhibits luminescence variation with sulfonation level of SPS. PL of QDs stabilized by SPS1 is mainly because of the exciton recombination, while that of SPS2 which is more than expected, is due to surface defect state emission at long wavelength region that competes with exciton recombination in blue region. The luminescence of SPS2 encapsulated CdS QD is dominated by emission from surface trap state whose intensity can be tuned by changing pH. The position of band edge emission peak is not disturbed by the sulfonation level of SPS, by the pH of the medium and on standing in aqueous solution. The SPS1 and SPS2 composites exhibit negative nonlinear refraction and nonlinear absorption with RSA to SA flip at focus. The nonlinear refractive index and the intensity of RSA and SA are decided by the QD surface interaction with the sulfonated polystyrene. Thus, the interesting surface nature dependent luminescence features and optical nonlinearity of the water-soluble QDs synthesized using a low cost method are proven. The great potential of the SPS-CdS composite lies in the fact that the sulfonate content can be altered to optimize the desired linear and nonlinear optical properties.

■ ASSOCIATED CONTENT

S Supporting Information

Synthesis of sulfonated polystyrene and its CdS QD composite. ¹H NMR spectrum of SPS2 to find the extent of sulfonation. HR-TEM images of SPS1-CdS and SPS2-CdS composite films suspended in THF. UV-vis absorption spectra of the composites at the time of CdS QD formation and on keeping in water for 3 h. PL of SPS2 in water. This material is available free of charge via the Internet at <http://pubs.acs.org>.

■ AUTHOR INFORMATION

Corresponding Author

*E-mail: principal@aisat.ac.in.

Present Address

^{II} Albertian Institute of Science and Technology, Cochin University P.O., Cochin, Kerala, India 682022.

Notes

The authors declare no competing financial interest.

■ ACKNOWLEDGMENTS

We gratefully thank DST unit of nanoscience, IIT Chennai for HR-TEM analysis and SAIF-STIC, CUSAT for diffuse reflectance spectroscopy. The financial support from University Grants Commission (UGC), India is also acknowledged.

■ REFERENCES

- (1) Lee, Y. H.; Chang, C. J.; Kao, C. J.; Dai, C. A. In Situ Template Synthesis of a Polymer/Semiconductor Nano hybrid Using Amphiphilic Conducting Block Copolymers. *Langmuir* **2010**, *26*, 4196–4206.
- (2) He, J.; Ji, W.; Ma, G. H.; Tang, S. H.; Kong, E. S. W.; Chow, S. Y.; Zhang, X. H.; Hua, Z. L.; Shi, J. L. Ultrafast and Large Third-Order Nonlinear Optical Properties of CdS Nanocrystals in Polymeric Film. *J. Phys. Chem. B* **2005**, *109*, 4373–4376.
- (3) Yu, L.; Ruan, H.; Zheng, Y.; Li, D. A Facile Solvothermal Method to Produce ZnS Quantum Dots-Decorated Graphene Nanosheets with Superior Photoactivity. *Nanotechnology* **2013**, *24*, 375601.
- (4) Lou, Y.; Zhao, Y.; Chen, J.; Zhu, J. J. Metal Ions Optical Sensing by Semiconductor Quantum Dots. *J. Mater. Chem. C* **2014**, *2*, 595–613.
- (5) Zhu, L.; Shi, Y.; Tu, C.; Wang, R.; Pang, Y.; Qiu, F.; Zhu, X.; Yan, D.; He, L.; Jin, C.; et al. Construction and Application of a pH-Sensitive Nanoreactor via a Double-Hydrophilic Multiarm Hyperbranched Polymer. *Langmuir* **2010**, *26*, 8875–8881.
- (6) Jia, L.; Xu, J. P.; Li, D.; Pang, S. P.; Fang, Y.; Song, Z. G.; Ji, J. Fluorescence Detection of Alkaline Phosphatase Activity with β -Cyclodextrin-Modified Quantum Dots. *Chem. Commun.* **2010**, *46*, 7166–7168.
- (7) Mansur, H. S.; Mansur, A. A. P. Fluorescent Nano hybrids: Quantum Dots Coupled to Polymer Recombinant Protein Conjugates for the Recognition of Biological Hazards. *J. Mater. Chem.* **2012**, *22*, 9006–9018.
- (8) Chen, N.; Zinchenko, A. A.; Yamazaki, Y.; Yoshikawa, Y.; Murata, S.; Yoshikawa, K. Quantum Dot Probes for Observation of Single Molecule DNA and a Synthetic Polyelectrolyte Higher-Order Structure. *Soft Matter* **2010**, *6*, 2834–2841.
- (9) Singh, S.; Garg, S.; Chahal, J.; Raheja, K.; Singh, D.; Singla, M. L. Luminescent Behavior of Cadmium Sulfide Quantum Dots for Gallic Acid Estimation. *Nanotechnology* **2013**, *24*, 115602.
- (10) Song, Y.; Luo, D.; Ye, S.; Huang, M.; Zhong, D.; Huang, Z.; Hou, H.; Wang, L. Spectroscopic Studies on the Interaction between EcoRI and CdS QDs and Conformation of EcoRI in EcoRI-CdS QDs Bi conjugates. *Phys. Chem. Chem. Phys.* **2012**, *14*, 16258–16266.
- (11) Amelia, M.; Flaminio, R.; Latterini, L. Recovery of CdS Nanocrystal Defects through Conjugation with Proteins. *Langmuir* **2010**, *26*, 10129–10134.
- (12) Zhuang, Z.; Lu, X.; Peng, Q.; Li, Y. Direct Synthesis of Water-Soluble Ultrathin CdS Nanorods and Reversible Tuning of the Solubility by Alkalinity. *J. Am. Chem. Soc.* **2010**, *132*, 1819–1821.
- (13) Celebi, S.; Erdamar, A. K.; Sennaroglu, A.; Kurt, A.; Acar, H. Y. Synthesis and Characterization of Poly(acrylic acid) Stabilized Cadmium Sulfide Quantum Dots. *J. Phys. Chem. B* **2007**, *111*, 12668–12675.
- (14) Huang, P.; Jiang, Q.; Yu, P.; Yang, L.; Mao, L. Alkaline Post-Treatment of Cd(II)-Glutathione Coordination Polymers: Towards Green Synthesis of Water-Soluble and Cytocompatible CdS Quantum Dots with Tunable Optical Properties. *ACS Appl. Mater. Interfaces* **2013**, *5*, 5239–5246.
- (15) Scherzel, R. E.; Spahr, K. B.; Kurmer, J. P.; Wood, V. E.; Jenkins, J. A. Nanocomposite Photonic Polymers. 1. Third-Order Nonlinear Optical Properties of Capped Cadmium Sulfide Nanocryst-

- als in an Ordered Polydiacetylene Host. *J. Phys. Chem. A* **1998**, *102*, 5622–5626.
- (16) Wang, Y.; Herron, N. Nanometer-Sized Semiconductor Clusters: Materials Synthesis, Quantum Size Effects, and Photophysical Properties. *J. Phys. Chem.* **1991**, *95*, 525–532.
- (17) Sheik-Bahae, M.; Said, A. A.; Wei, T. H.; Hagan, D. J.; Stryland, E. W. V. Sensitive Measurement of Optical Nonlinearities Using a Single Beam. *IEEE J. Quantum Electron.* **1990**, *26*, 760–769.
- (18) Patete, J. M.; Peng, X.; Koenigsmann, C.; Xu, Y.; Karn, B.; Wong, S. S. Viable Methodologies for the Synthesis of High-Quality Nanostructures. *Green Chem.* **2011**, *13*, 482–519.
- (19) Baigl, D.; Seery, T. A. P.; Williams, C. E. Preparation and Characterization of Hydrosoluble, Partially Charged Poly(styrenesulfonate)s of Various Controlled Charge Fractions and Chain Lengths. *Macromolecules* **2002**, *35*, 2318–2326.
- (20) Antony, J. V.; Kurian, P.; Vadakkedathu, N. P. N.; Kochimoolayil, G. E. In Situ Synthesis of CdS Quantum Dot-Partially Sulfonated Polystyrene Composite: Characterization and Optical Properties. *Ind. Eng. Chem. Res.* **2014**, *53*, 2261–2269.
- (21) Langford, J. I.; Wilson, A. J. C. Scherrer after Sixty Years: A Survey and Some New Results in the Determination of Crystallite Size. *J. Appl. Crystallogr.* **1978**, *11*, 102–113.
- (22) Moffitt, M.; Eisenberg, A. Size Control of Nanoparticles in Semiconductor-Polymer Composites. 1. Control via Multiplet Aggregation Numbers in Styrene-Based Random Ionomers. *Chem. Mater.* **1995**, *7*, 1178–1184.
- (23) Yang, J. C.; Jablonsky, M. J.; Mays, J. W. NMR and FTIR Studies of Sulfonated Styrene-Based Homopolymers and Copolymers. *Polymer* **2002**, *43*, 5125–5132.
- (24) Cullity, B. D. *Elements of X-ray Diffraction*; Addison-Wesley: New York, 1977.
- (25) Sekhar, H.; Rao, D. N. Stokes and Anti-Stokes Luminescence in Heat-Treated CdS Nanopowders. *J. Phys. Chem. C* **2013**, *117*, 2300–2307.
- (26) Vempati, S.; Ertas, Y.; Uyar, T. Sensitive Surface States and their Passivation Mechanism in CdS Quantum dots. *J. Phys. Chem. C* **2013**, *117*, 21609–21618.
- (27) Du, H.; Xu, G. Q.; Chin, W. S. Synthesis, Characterization, and Nonlinear Optical Properties of Hybridized CdS-Polystyrene Nanocomposites. *Chem. Mater.* **2002**, *14*, 4473–4479.
- (28) Sahiner, N.; Sel, K.; Meral, K.; Onganer, Y.; Butun, S.; Ozay, O.; Silan, C. Hydrogel Templated CdS Quantum Dots Synthesis and their Characterization. *Colloids Surf., A* **2011**, *389*, 6–11.
- (29) Azevedo, W. M.; Menezes, F. D. A New and Straightforward Synthesis Route for Preparing CdS Quantum Dots. *J. Lumin.* **2012**, *132*, 1740–1743.
- (30) Moffitt, M.; McMohan, L.; Pessel, V.; Eisenberg, A. Size Control of Nanoparticles in Semiconductor-Polymer Composites. 2. Control via Sizes of Spherical Ionic Microdomains in Styrene-Based Diblock Ionomers. *Chem. Mater.* **1995**, *7*, 1185–1192.
- (31) Gao, Y.; Tonizzo, A.; Walser, A.; Potasek, M.; Dorsinvile, R. Enhanced Optical Nonlinearity of Surfactant-Capped CdS Quantum Dots Embedded in an Optically Transparent Polystyrene Thin Film. *Appl. Phys. Lett.* **2008**, *92*, 033106.
- (32) Karan, S.; Majumder, M.; Mallik, B. Controlled Surface Trap State Photoluminescence from CdS QDs Impregnated in Poly(methyl methacrylate). *Photochem. Photobiol. Sci.* **2012**, *11*, 1220–1232.
- (33) Baker, D. R.; Kamat, P. V. Tuning the Emission of CdSe Quantum Dots by Controlled Trap Enhancement. *Langmuir* **2010**, *26*, 11272–11276.
- (34) Wang, C. W.; Moffitt, M. G. Surface-Tunable Photoluminescence from Block Copolymer-Stabilized Cadmium Sulfide Quantum Dots. *Langmuir* **2004**, *20*, 11784–11796.
- (35) Karan, S.; Mallik, B. Tunable Visible-Light Emission from CdS Nanocrystallites Prepared under Microwave Irradiation. *J. Phys. Chem. C* **2007**, *111*, 16734–16741.
- (36) Pradeep, C.; Mathew, S.; Nithyaja, B.; Radhakrishnan, P.; Nampoori, V. P. N. Studies of Nonlinear Optical Properties of Picogreen Dye using Z-Scan Technique. *Appl. Phys. A: Mater. Sci. Process.* **2014**, *115*, 291–295.
- (37) Li, H. P.; Kam, C. H.; Lam, Y. L.; Ji, W. Optical Nonlinearities and Photo-Excited Carrier Life Time in CdS at 532 nm. *Opt. Commun.* **2001**, *190*, 351–356.
- (38) Krauss, T. D.; Wise, F. W. Femtosecond Measurement of Nonlinear Absorption and Refraction in CdS, ZnSe, and ZnS. *Appl. Phys. Lett.* **1994**, *65*, 1739–1741.
- (39) Wang, Y.; Herron, N.; Mahler, W.; Suna, A. Linear and Nonlinear Optical Properties of Semiconductor Clusters. *J. Opt. Soc. Am. B* **1989**, *6*, 808–813.
- (40) Rojo, R. R.; Stranges, L.; Kar, A. K.; Rojas, M. A. M.; Watson, W. H. Saturation in the Near-Resonance Nonlinearities in a Triazole-Quinone Derivative. *Opt. Commun.* **2002**, *203*, 385–391.
- (41) Zhu, X. R.; Sun, Z. R.; Niu, R. M.; Zeng, H. P.; Wang, Z. G.; Lang, J. P.; Xu, Z. Z.; Li, R. X. Optical Nonlinear Properties and Optical Limiting for [(n-Bu)₄N]₄[MoS₄Cu]₄. *J. Appl. Phys.* **2003**, *94*, 4772–4775.
- (42) Cassano, T.; Tommasi, R.; Meacham, A. P.; Ward, M. D. Investigation of the Excited-State Absorption of a Ru Dioxolene Complex by the Z-Scan Technique. *J. Chem. Phys.* **2005**, *122*, 154507.
- (43) Nithyaja, B.; Misha, H.; Radhakrishnan, P.; Nampoori, V. P. N. Effect of Deoxyribonucleic Acid on Nonlinear Optical Properties of Rhodamine 6G-Polyvinyl Alcohol Solution. *J. Appl. Phys.* **2011**, *109*, 023110.
- (44) Asunkis, D. J.; Bolotin, I. L.; Hanley, L. Nonlinear Optical Properties of PbS Nanocrystals Grown in Polymer Solutions. *J. Phys. Chem. C* **2008**, *112*, 9555–9558.
- (45) Pradeep, C.; Mathew, S.; Nithyaja, B.; Radhakrishnan, P.; Nampoori, V. P. N. Effect of Marine Derived Deoxyribonucleic Acid on Nonlinear Optical Properties of PicoGreen Dye. *Appl. Phys. B: Laser Opt.* **2013**, *111*, 611–615.